OPEN

Citation: Cell Death and Disease (2014) 5, e1168; doi:10.1038/cddis.2014.138

www.nature.com/cddis

Constitutive expression of murine c-FLIP$_R$ causes autoimmunity in aged mice

F Ewald[1,2], M Annemann[1,2], MC Pils[3], C Plaza-Sirvent[1,2], F Neff[4], C Erck[5], D Reinhold[1] and I Schmitz*[,1,2]

Death receptor-mediated apoptosis is a key mechanism for the control of immune responses and dysregulation of this pathway may lead to autoimmunity. Cellular FLICE-inhibitory proteins (c-FLIPs) are known as inhibitors of death receptor-mediated apoptosis. The only short murine c-FLIP splice variant is c-FLIP$_{Raji}$ (c-FLIP$_R$). To investigate the functional role of c-FLIP$_R$ in the immune system, we used the vavFLIP$_R$ mouse model constitutively expressing murine c-FLIP$_R$ in all hematopoietic compartments. Lymphocytes from these mice are protected against CD95-mediated apoptosis and activation-induced cell death. Young vavFLIP$_R$ mice display normal lymphocyte compartments, but the lymphocyte populations alter with age. We identified reduced levels of T cells and slightly higher levels of B cells in 1-year-old vavFLIP$_R$ mice compared with wild-type (WT) littermates. Moreover, both B and T cells from aged vavFLIP$_R$ animals show activated phenotypes. Sera from 1-year-old WT and transgenic animals were analysed for anti-nuclear antibodies. Notably, elevated titres of these autoantibodies were detected in vavFLIP$_R$ sera. Furthermore, tissue damage in kidneys and lungs from aged vavFLIP$_R$ animals was observed, indicating that vavFLIP$_R$ mice develop a systemic lupus erythematosus-like phenotype with age. Taken together, these data suggest that c-FLIP$_R$ is an important modulator of apoptosis and enforced expression leads to autoimmunity.

Cell Death and Disease (2014) **5,** e1168; doi:10.1038/cddis.2014.138; published online 10 April 2014
Subject Category: Immunity

It is crucial that excessive lymphocytes are deleted by apoptosis after efficient antigen clearance to maintain cell homeostasis.[1] Moreover, insufficient apoptosis of auto-reactive immune cells may result in autoimmune diseases.[1] The extrinsic apoptosis pathway is triggered by ligand binding of death receptors, such as CD95 (Fas/APO-1), and regulates the removal of unwanted lymphocytes.[2] Elimination of T cells is achieved by activation-induced cell death (AICD), which is triggered upon restimulation of T cells without co-stimulation.[2] Notably, the CD95 death receptor pathway was shown to be important for AICD.[3–6] Furthermore, dysregulation of the CD95 signalling pathway was reported to result in severely altered lymphoproliferation (Lpr) and autoimmunity in both *lpr* and *generalised lymphoproliferative disorder* (*gld*) mice, which have mutated CD95 receptor or ligand, respectively, as well as in patients suffering from the homologous human disease autoimmune lymphoproliferative syndrome.[7,8] CD95 is the best-characterised death receptor and it is activated by binding of its cognate ligand CD95L.[9] Ligand-binding results in receptor oligomerisation and formation of the death-inducing signalling complex (DISC) through recruitment of the proteins Fas-associated death domain-containing protein (FADD), procaspase-8, -10 and cellular FLICE-inhibitory protein (c-FLIP).[10] Autoproteolytic processing of procaspase-8 at the DISC generates active caspase-8,[11,12] which cleaves and activates caspase-3 and -7. The effector caspases process further substrates, eventually leading to apoptosis.[13,14] The c-FLIPs inhibit apoptosis by competing with procaspase-8 for binding sites at the DISC and additionally interfere with caspase-8 processing.[15–17] So far, three c-FLIP isoforms expressed on the protein level have been reported: c-FLIP$_{Long}$ (c-FLIP$_L$), c-FLIP$_{Short}$ (c-FLIP$_S$) and c-FLIP$_{Raji}$ (c-FLIP$_R$).[15,17,18] The long isoform resembles caspase-8, but lacks catalytic function because of substitution of amino-acid residues critical for enzymatic activity.[18,19] The two short isoforms are distinguished by a functional nucleotide polymorphism and mainly consist of the death effector domains with unique C-terminal tails.[20] The structure of the murine

[1]Institute of Molecular and Clinical Immunology, Otto-von-Guericke-University Magdeburg, Leipziger Str. 44, Magdeburg, Germany; [2]Research Group of Systems-Oriented Immunology and Inflammation Research, Department of Immune Control, Helmholtz Centre for Infection Research, Inhoffenstr. 7, Braunschweig, Germany; [3]Mouse Pathology, Animal Experimental Unit, Helmholtz Centre for Infection Research, Inhoffenstr. 7, Braunschweig, Germany; [4]Institute of Pathology, Helmholtz Centre Munich, Ingolstaedter Landstr. 1, Neuherberg, Germany and [5]Cellular Proteome Research, Department of Structure and Function of Proteins, Helmholtz Centre for Infection Research, Inhoffenstr. 7, Braunschweig, Germany
*Corresponding author: I Schmitz, Institute of Molecular and Clinical Immunology, Otto-von-Guericke-University Magdeburg, Leipziger Str. 44, Magdeburg, Germany or Research Group of Systems-Oriented Immunology and Inflammation Research, Department of Immune Control, Helmholtz Centre for Infection Research, Inhoffenstr. 7, D-38124, Braunschweig, Germany. Tel: +49 531 61813500; Fax: +49 531 61813599; E-mail: ingo.schmitz@helmholtz-hzi.de
Keywords: c-FLIP; apoptosis; CD95; autoimmunity
Abbreviations: AICD, activation-induced cell death; ANA, anti-nuclear antibody; BALT, bronchial-associated lymphoid tissue; *Cflar*, caspase-8 and FADD-like apoptosis regulator; c-FLIP$_L$, cellular FLICE-inhibitory protein, long isoform; c-FLIP$_S$, cellular FLICE-inhibitory protein, short isoform; c-FLIP$_R$, cellular FLICE-inhibitory protein, Raji isoform; CNS, central nervous system; DC, dendritic cell; DISC, death-inducing signalling complex; DN, double negative; EAE, experimental autoimmune encephalomyelitis; FADD, Fas-associated death domain-containing protein; *Gld*, generalised lymphoproliferative disorder; IFN-γ, interferon-γ; *Lpr*, lymphoproliferation; MOG, myelin oligodendrocyte glycoprotein; MS, multiple sclerosis; SLE, systemic lupus erythematosus; WT, wild type
Received 05.9.13; revised 27.2.14; accepted 28.2.14; Edited by M Leverkus

Cflar (*caspase-8 and FADD-like apoptosis regulator*) gene differs from the human gene locus, in that only c-FLIP$_L$ and c-FLIP$_R$ can be expressed.[21] Although the short c-FLIP isoforms have been described as anti-apoptotic, c-FLIP$_L$ was reported to act both pro- and anti-apoptotic depending on expression level and strength of receptor stimulation.[22–24] Transgenic overexpression of c-FLIP$_L$ in mice resulted in autoimmunity, although only in the Balb/c background.[25] In contrast, mice overexpressing human c-FLIP$_S$ did not develop autoimmune disease.[26,27] Not much is known about the physiological function of c-FLIP$_R$. To investigate the functional role of c-FLIP$_R$ in the immune system, we used a mouse model, called vavFLIP$_R$, with constitutive expression of murine c-FLIP$_R$ in all hematopoietic compartments. We previously reported that these transgenic mice have a better clearance of the Gram-positive bacteria *Listeria monocytogenes* compared with infected wild-type (WT) mice.[28] Here we show that aged mice constitutively expressing murine c-FLIP$_R$ have altered lymphocyte populations with higher levels of activated B and T cells compared with WT littermates. Moreover, vavFLIP$_R$ animals spontaneously develop autoimmunity with age, showing features of systemic lupus erythematosus (SLE).

Results

vavFLIP$_R$ mice do not recapitulate the *lpr*/*gld* phenotype. Insufficient cell death can lead to autoimmunity as a result of altered immune cell populations. *Lpr* and *gld* mice, with mutations in the CD95 receptor and ligand, respectively, develop Lpr and autoimmunity.[7,29] Moreover, these mice accumulate unusual CD4$^-$ CD8$^-$ double negative (DN) B220$^+$ $\alpha\beta$ T cells.[7,30] c-FLIP$_R$ inhibits apoptosis by competing with caspase-8 for binding sites at the DISC.[17,21] The mouse model vavFLIP$_R$, in which murine c-FLIP$_R$ is under control of the *vav*-promoter to ensure expression in all hematopoietic compartments,[28] was used to study the functional role of murine c-FLIP$_R$ in the immune system. As thymocytes as well as B and T cells from vavFLIP$_R$ mice were protected against CD95-induced apoptosis,[28] we investigated if the impaired lymphocyte apoptosis in vavFLIP$_R$ mice would lead to elevated numbers of lymphocytes and altered lymphocyte populations with age. No Lpr was identified in 12–14 months old vavFLIP$_R$ animals. In fact, the number of cells in the peripheral lymph nodes (pLNs) from vavFLIP$_R$ mice was reduced compared with WT littermates (Figure 1a). Furthermore, pLN cells of WT and vavFLIP$_R$ mice were analysed for DN B220$^+$ T cells compared with 3 months old MRL/*lpr* mice as controls. The characteristic DN B220$^+$ population was identified in MRL/*lpr* mice, but was not observed in either WT or vavFLIP$_R$ animals (Figure 1b). The lack of DN B220$^+$ T cells in vavFLIP$_R$ mice is similar to the phenotype of c-FLIP$_L$ transgenic mice[31] and mice with transgenic expression of human c-FLIP$_S$.[27] Thus, vavFLIP$_R$ mice do not develop an *lpr*/*gld*-like phenotype.

Altered lymphocyte populations in aged vavFLIP$_R$ mice. Young vavFLIP$_R$ mice displayed normal lymphocyte populations.[28] We analysed aged WT and vavFLIP$_R$ mice to investigate if the constitutive expression of c-FLIP$_R$ alters lymphocyte populations over time. Dendritic cells (DCs), macrophages and granulocytes have been reported to be regulated through death receptors and c-FLIP proteins.[32,33] We therefore analysed the frequencies of CD11c$^+$ DCs,

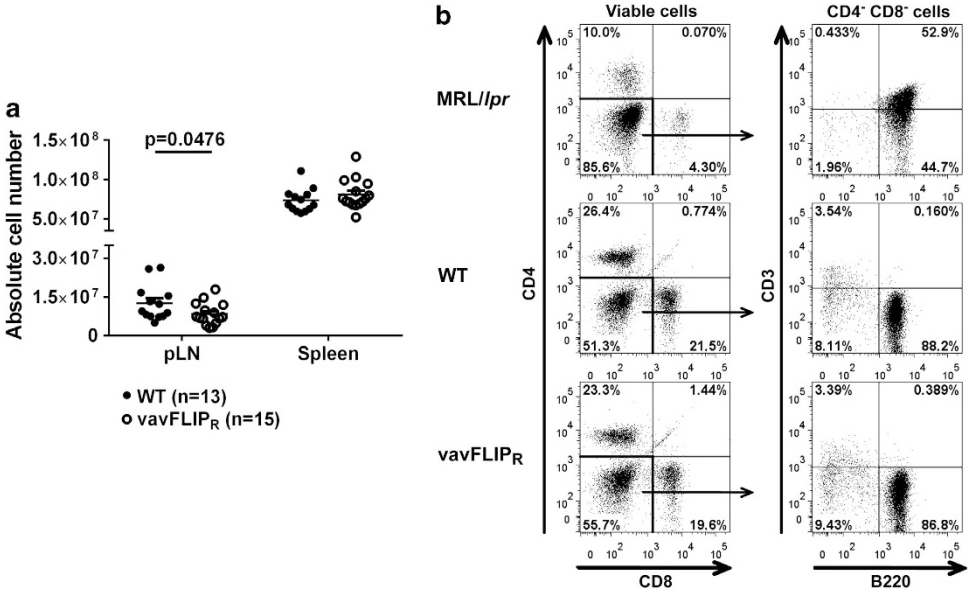

Figure 1 One-year-old vavFLIP$_R$ mice display normal cellularity in lymphoid organs and do not accumulate DN B220$^+$ cells. (**a**) Absolute cell numbers in pLNs and spleens of WT ($n=13$) and vavFLIP$_R$ ($n=15$) mice at 12–14 months of age. Symbols represent individual mice, horizontal lines display the mean ± S.E.M. pooled from five independent experiments. Statistical analysis was performed with two-tailed nonparametric Mann–Whitney *U*-test. (**b**) Analysis of DN B220$^+$ cells in pLNs from 1-year-old WT and vavFLIP$_R$ animals. Representative dot plots are shown for MRL/*lpr* ($n=2$), WT ($n=6$) and vavFLIP$_R$ ($n=7$) mice. Three months old MRL/*lpr* mice develop the characteristic DN B220$^+$ cells (upper panel). This subset could not be identified in either WT (mid panel) or vavFLIP$_R$ mice (lower panel)

CD49b$^+$ natural killer (NK) cells, F4/80$^+$ macrophages and Gr1$^+$ granulocytes in 1-year-old mice. The populations of CD11c$^+$, CD49b$^+$, F4/80$^+$ and Gr1$^+$ cells from WT and vavFLIP$_R$ were comparable (Supplementary Table 1). Flow cytometry analyses of lymphocyte sub-populations in spleen and pLNs from 12 to 14 months old mice revealed reduced frequencies of vavFLIP$_R$ CD3$^+$ T cells compared with WT CD3$^+$ T cells (Figures 2a and b), consistent with reduced absolute CD3$^+$ T-cell number in pLNs from vavFLIP$_R$ animals (Figure 2c). Furthermore, an increased percentage of vavFLIP$_R$ CD19$^+$ B cells in pLNs compared with WT was observed (Figures 2a and d). Frequencies and absolute numbers of CD19$^+$ B cells were not significantly altered in the spleen (Figure 2e). Neither did we detect alterations in germinal centre formation in aged transgenic mice (data not shown). The CD4$^+$/CD8$^+$ cell profiles within the CD3$^+$ T-cell compartment were comparable between WT and vavFLIP$_R$ mice (Supplementary Figure 1). Nevertheless, lower frequencies of splenic CD8$^+$ T cells were observed as well as reduced absolute cell numbers of CD8$^+$ cells in pLNs (Supplementary Figure 1b). As we previously reported that thymocyte development in vavFLIP$_R$ mice is normal,[28] we suggest that c-FLIP$_R$ expression regulates homeostasis of peripheral CD8$^+$ T cells. Taken together, the B- and T-cell populations are altered in aged vavFLIP$_R$ mice, whereas other haematopoietic cells are unaffected.

Activated phenotypes of T and B cells from vavFLIP$_R$ mice. The activation status of T cells in young vavFLIP$_R$ mice was comparable to WT littermates.[28] As AICD is impaired in T cells from vavFLIP$_R$ mice,[28] we investigated if the activation status changed with age. We observed higher percentages of vavFLIP$_R$ CD4$^+$ cells expressing the activation marker CD25 in comparison with WT CD4$^+$ cells (Figures 3a and b), with absolute cell numbers being similar between 12 and 14 months old WT and vavFLIP$_R$ mice (Figure 3c). As CD25 is not only a marker for activated T cells, but is also highly expressed on regulatory T (T$_{reg}$) cells,[34] we analysed the expression of the master transcription factor of T$_{reg}$ cells, Foxp3.[35] Indeed, most of the CD25$^+$ CD4$^+$ T cells co-expressed Foxp3 indicating that 1-year-old vavFLIP$_R$ mice have higher levels of T$_{reg}$ cells in both pLNs (Figure 3d) and spleen (data not shown) compared with WT littermates. Interestingly, we also observed an increase in CD25$^+$ T cells that were negative for Foxp3 suggesting that

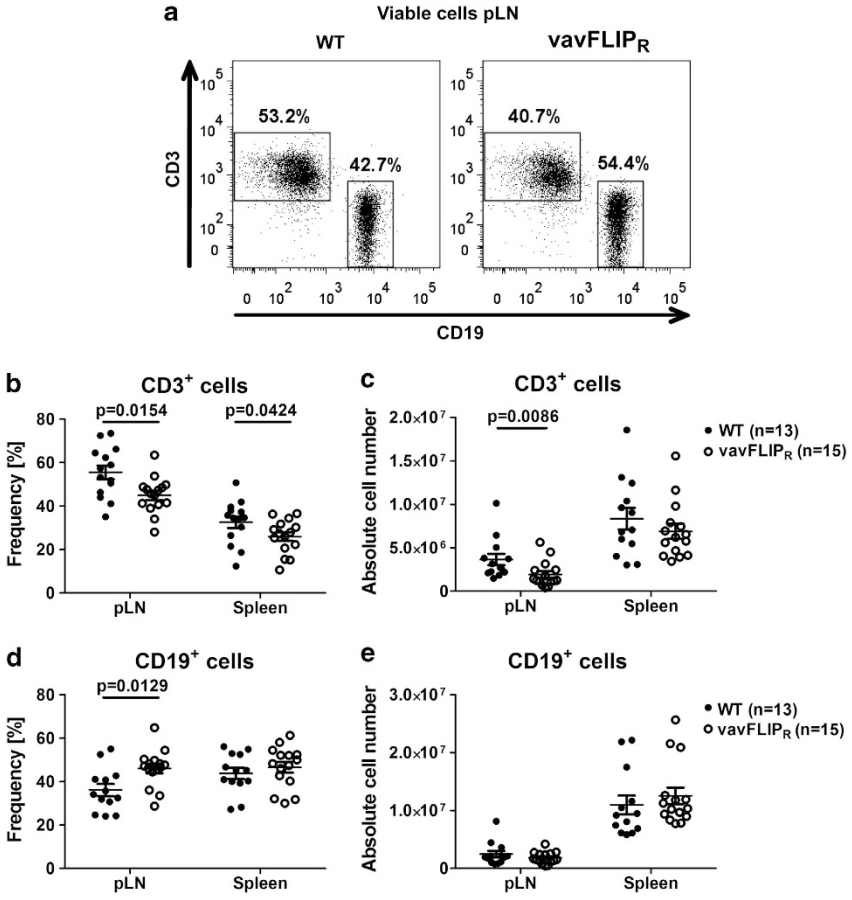

Figure 2 Altered lymphocyte populations in 12–14 months old vavFLIP$_R$ mice. (**a**) Representative dot plots of CD3- and CD19-stained WT and vavFLIP$_R$ pLN cells. Frequency and absolute cell number of CD3$^+$ cells (**b** and **c**) and CD19$^+$ cells (**d** and **e**) in freshly isolated pLNs and spleens from WT ($n=13$) and vavFLIP$_R$ ($n=15$) littermates. Individual mice are represented as separate symbols. Horizontal lines show the mean pooled from five independent experiments; error bars display the S.E.M. Statistical analyses were performed with two-tailed nonparametric Mann–Whitney *U*-tests

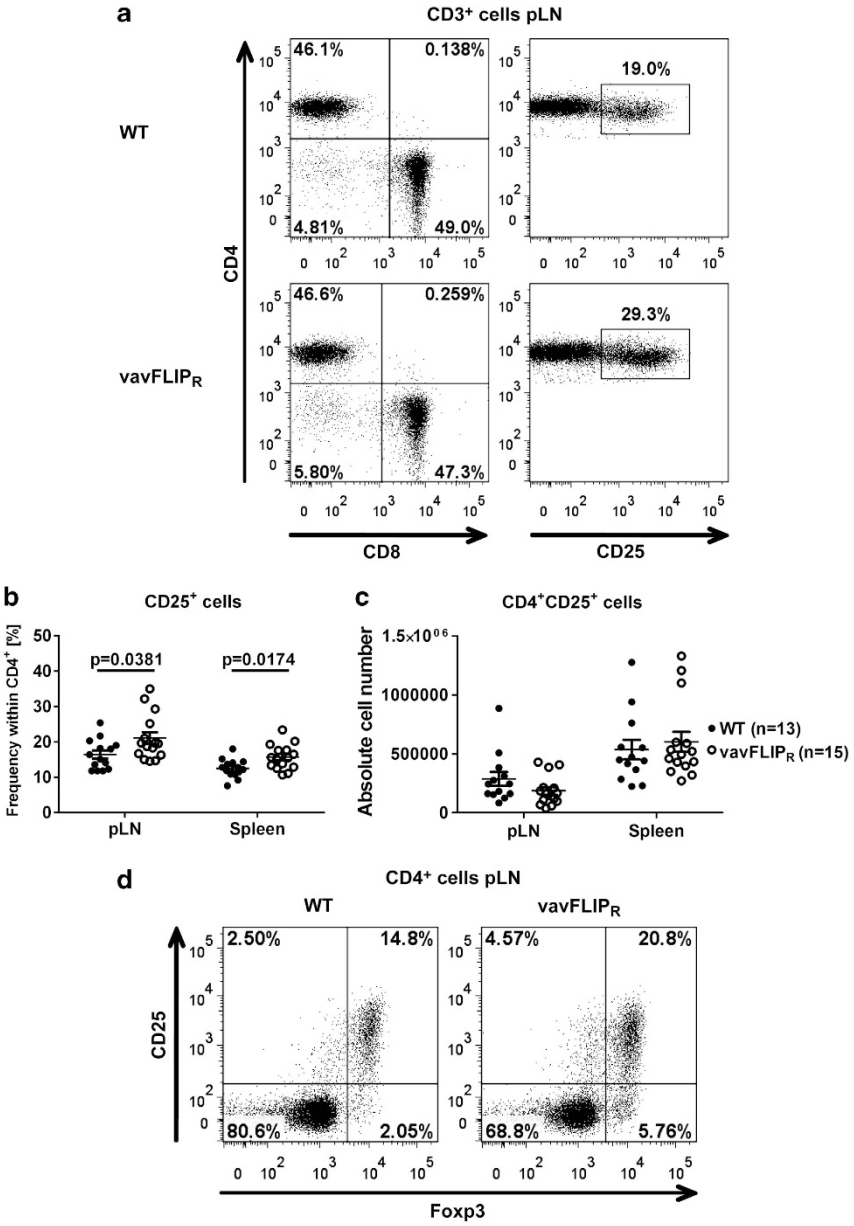

Figure 3 Increased levels of CD25$^+$ T cells and T_{reg} cells in 1-year-old vavFLIP$_R$ animals. (**a**) Representative dot plots of WT (upper panel) and vavFLIP$_R$ (lower panel) CD3$^+$ cells in pLNs. Frequency (**b**) and absolute cell number (**c**) of CD4$^+$CD25$^+$ cells in WT ($n = 13$) and vavFLIP$_R$ ($n = 15$) pLN and spleens. Symbols represent individual mice. Horizontal lines display the mean ± S.E.M. Statistical analyses were performed with two-tailed nonparametric Mann–Whitney *U*-tests. (**d**) Dot plots showing CD25$^+$ and Foxp3$^+$ T cells within the CD4$^+$ compartment representative for three WT (left) and four vavFLIP$_R$ (right) mice

conventional T cells may indeed be more activated (Figure 3d). Therefore, the memory/naive T-cell profile was analysed in 12–14 months old WT and vavFLIP$_R$ animals. Strikingly, elevated frequencies of CD44$^+$ antigen-experienced cells within the CD3$^+$ compartment were identified in both pLNs and spleen from vavFLIP$_R$ mice (Figures 4a and b). We also observed reduced numbers of CD3$^+$CD62L$^+$ naive T cells in vavFLIP$_R$ animals (Supplementary Figure 2a). Notably, both within the CD4$^+$ helper T-cell population and the CD8$^+$ cytotoxic T-cell population from vavFLIP$_R$ pLNs and spleens, higher levels of antigen-experienced (CD44$^+$) cells and lower levels of naive (CD62L$^+$) cells were identified compared with WT (Figures 4c and d). The absolute cell numbers of CD62L$^+$ cells were reduced for both CD4$^+$ and CD8$^+$ T-cell populations (Supplementary Figures 2b and c). These data indicate that T cells from vavFLIP$_R$ mice are highly activated in comparison with WT T cells.

Similar to T cells, B cells from vavFLIP$_R$ mice are protected against apoptosis.[28] The activation status of B cells was examined by flow cytometry. CD40, CD80 and CD95 had similar expression levels in vavFLIP$_R$ and WT animals (data not shown), whereas analysis of the activation markers CD69, CD86 and major histocompatibility complex class II molecule

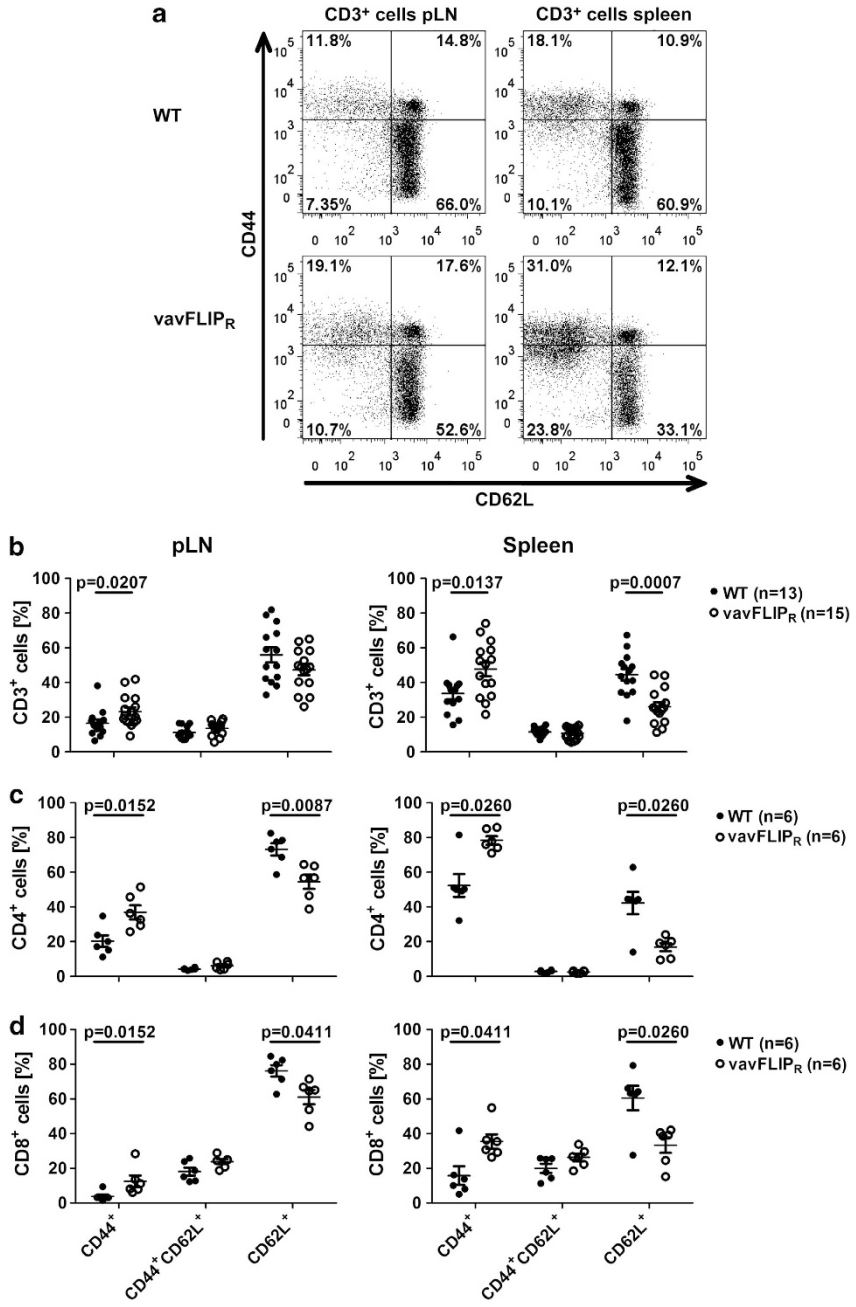

Figure 4 T cells from vavFLIP$_R$ mice at 12–14 months of age are highly activated. (**a**) Representative dot plots of pLN cells (left panel) and splenocytes (right panel) from WT (upper panel) and vavFLIP$_R$ animals (lower panel). Frequencies of CD44$^+$, CD44$^+$CD62L$^+$ and CD62L$^+$ cells within CD3$^+$ cells (**b**), CD4$^+$ cells (**c**) and CD8$^+$ cells (**d**) from pLN and spleen. (**b-d**) Symbols represent individual WT (**b**: $n = 13$, **c** and **d**: $n = 6$) and vavFLIP$_R$ (**b**: $n = 15$, **c** and **d**: $n = 6$) mice. Horizontal lines represent (**b**) the mean pooled from five independent experiments or (**c** and **d**) the mean of one experiment representative for two independent experiments; error bars display S.E.M. Statistical analyses were performed with two-tailed nonparametric Mann–Whitney *U*-tests

I-A/I-E revealed an increased expression of these markers in vavFLIP$_R$ B cells compared with WT B cells (Figure 5). This indicates that B cells from 12 to 14 months old vavFLIP$_R$ mice are more activated in comparison with B cells from WT animals at 1 year of age. The activated phenotypes of B and T cells identified in 1-year-old vavFLIP$_R$ mice are consistent with a previous study, which reported that B and T cells from c-FLIP$_L$ transgenic mice on a Balb/c background were highly activated.[25]

Disease progression in MOG-EAE is comparable between WT and vavFLIP$_R$ mice. As constitutive expression of c-FLIP$_R$ alters lymphocyte populations and activation status with age, we investigated if this has functional relevance in T-cell-mediated autoimmune disease. Experimental autoimmune encephalomyelitis (EAE) is a widely accepted animal model for studying the human demyelinating inflammatory disorder multiple sclerosis (MS).[36] T_H1 and T_H17 effector T cells have been shown to

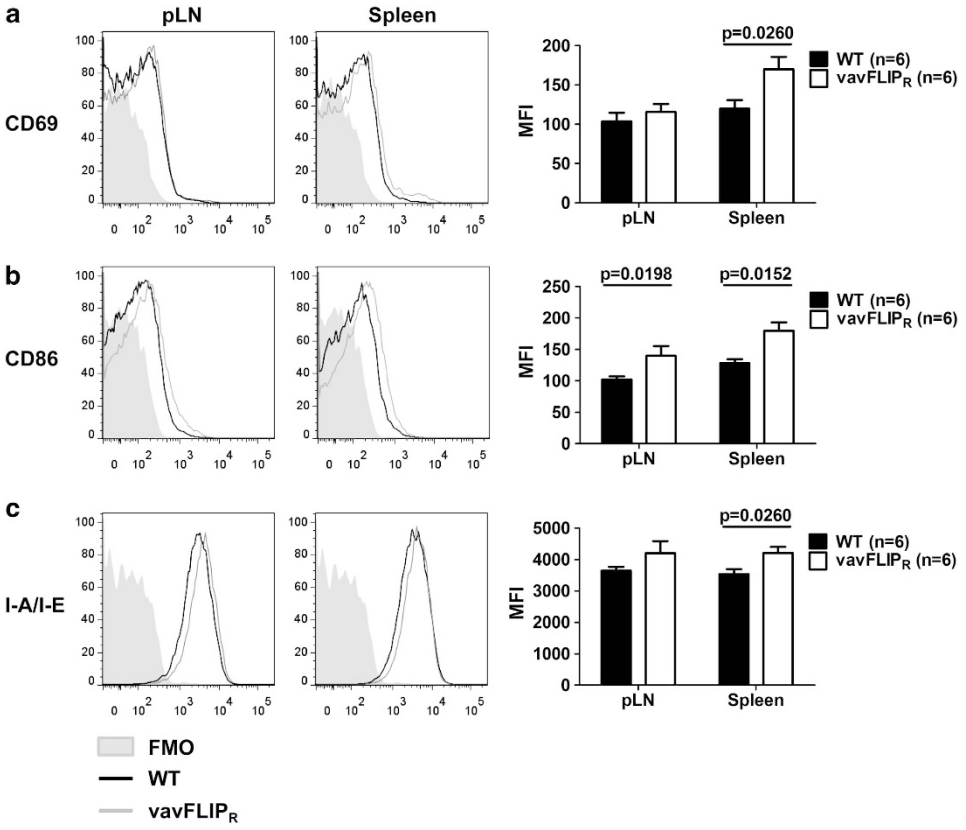

Figure 5 vavFLIP$_R$ B cells from 12 to 14 months old mice show an activated phenotype. (**a**–**c**) pLN cells and splenocytes from WT and vavFLIP$_R$ mice ($n=6$) were isolated and analysed by flow cytometry. The activation status of CD19$^+$ B cells was assayed by the markers CD69 (**a**), CD86 (**b**) and I-A/I-E (**c**). Representative histograms with fluorescent minus one (FMO) as control (left panel) and diagrams displaying the mean fluorescent intensity (MFI; right panel) ± S.E.M. are shown. Statistical analyses were performed with two-tailed nonparametric Mann–Whitney *U*-tests

contribute to the pathology in EAE[37] and c-FLIP$_L$ transgenic mice were reported to be resistant to myelin oligodendrocyte glycoprotein (MOG)-EAE because of enhanced T_H2, and thus diminished T_H1, effector responses.[38] To assess if c-FLIP$_R$ influences the differentiation of T_H0, T_H1, T_H2 or T_H17 cells, we cultured naive WT and vavFLIP$_R$ T cells under T_H1, T_H2 or T_H17 polarising conditions *in vitro*. The frequencies of interferon-γ (IFN-γ)-producing T_H1 cells were comparable between WT and vavFLIP$_R$ differentiated T cells (Figures 6a and b). Interestingly, frequencies in IL-17A-producing T_H17 cells and IL-4 mRNA induction in T_H2 cells were lower in vavFLIP$_R$ T cells cultured under the respective polarising conditions (Figures 6a, b and c).

WT and vavFLIP$_R$ mice were immunised with the MOG$_{35-55}$ peptide in complete Freund's adjuvant in conjunction with pertussis toxin to investigate if constitutive murine c-FLIP$_R$ expression in T cells, macrophages and DCs influences EAE disease. However, both WT and vavFLIP$_R$ animals developed disease with neurological defects resulting in paralysis of the tail and muscle weakness with comparable severity of disease. Only a slightly slower disease progression was observed in vavFLIP$_R$ mice (Figure 6d). To investigate whether T-cell effector responses were affected by the transgenic expression of c-FLIP$_R$ *in vivo*, we analysed cytokine production in MOG-peptide restimulated T cells from MOG-immunised mice. We observed slightly reduced frequencies of IFN-γ^+ and IL-17A$^+$ cells from vavFLIP$_R$ pLNs in comparison with WT 11 days after immunisation (Figure 6e). This effect was levelled out at higher MOG peptide concentrations on day 14 (Figure 6e). The frequencies of IL-4-producing T cells in pLNs from vavFLIP$_R$ and WT mice were comparable (Figure 6e). Similar results were obtained when T cells were restimulated in a polyclonal manner, that is, with anti-CD3 and anti-CD28 (Supplementary Figure 3). In summary, our data indicate a minor defect in vavFLIP$_R$ effector T-cell responses that results in a slight delay in EAE disease progression in vavFLIP$_R$ mice.

Elevated ANA-titres and tissue damage of kidneys and lungs in aged vavFLIP$_R$ mice. B-cell-mediated autoimmunity is characterised by autoantibodies targeting the body's own tissues. As vavFLIP$_R$ mice had slightly higher B-cell levels with activated phenotype, we analysed sera from 1-year-old WT and vavFLIP$_R$ mice for anti-nuclear antibodies (ANAs) using an indirect immunofluorescence assay with HEp-2 cells as source of nuclear antigens. Negative fluorescent pattern was most often observed when sera from WT mice were incubated on HEp-2 cells (Figure 7a), whereas homogenous fluorescent pattern was detected for the majority of sera from vavFLIP$_R$ mice even at high serum dilution (Figure 7b). Hence, significantly more

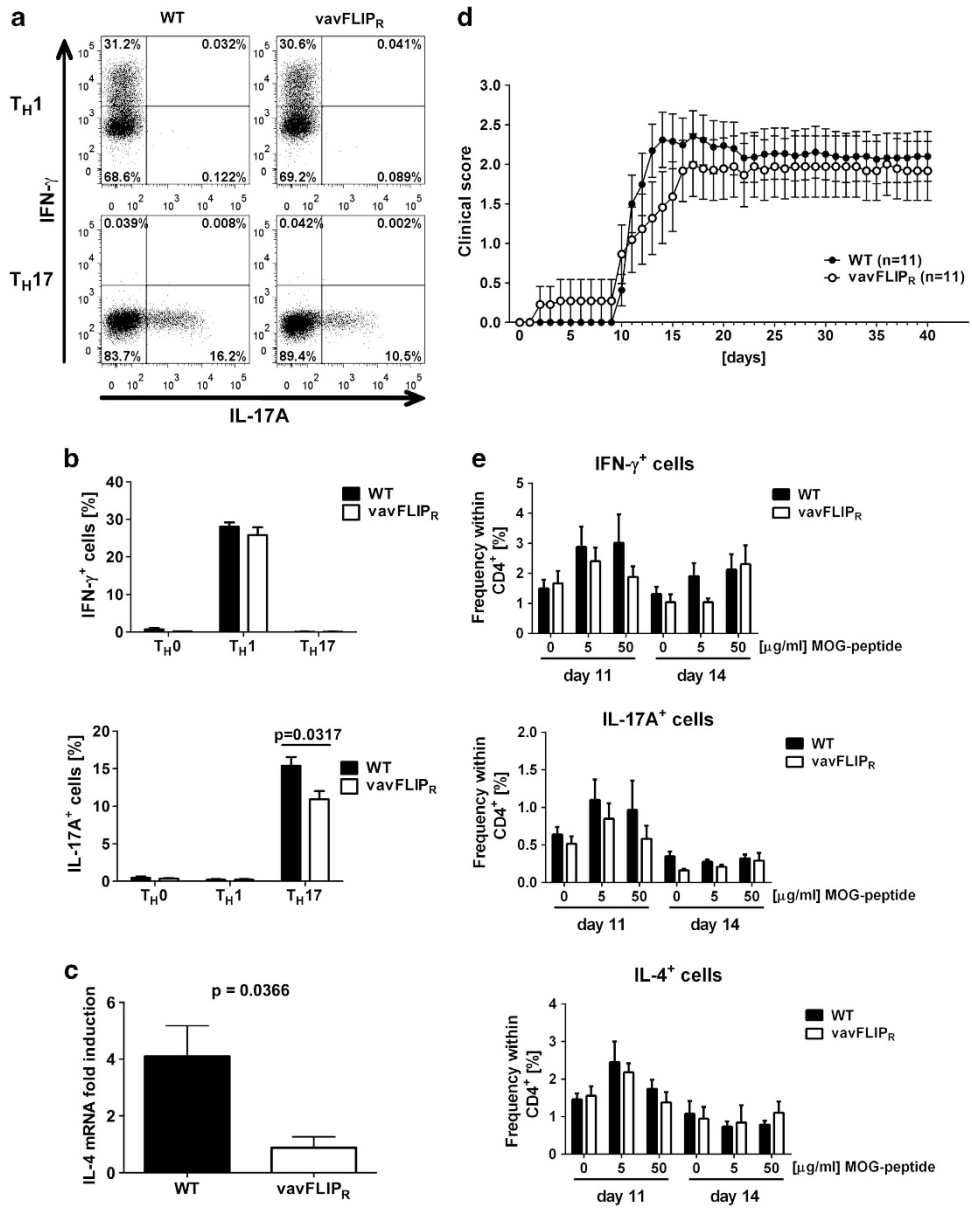

Figure 6 Comparable disease progression in MOG_{35-55}-peptide-induced EAE in WT and vavFLIP$_R$ mice. (**a**–**c**) Naive T cells from WT and vavFLIP$_R$ mice were isolated and cultured under T_H0, T_H1, T_H2 and T_H17 polarising conditions, followed by flow cytometry analysis of IFN-γ and IL-17A. (**a**) Representative dot plots of T_H1 and T_H17 differentiated cells are shown. (**b**) Data are represented as the mean ± S.E.M. from two independent experiments ($n = 5$ for WT and vavFLIP$_R$ cells). Statistical analyses were performed with two-tailed nonparametric Mann–Whitney *U*-tests. (**c**) Quantitative real-time PCR analysis of IL-4 mRNA expression in TH2 differentiated WT and vavFLIP$_R$ T cells. Data are represented as the mean ± S.E.M. from two independent experiments ($n = 4$ for WT and $n = 5$ for vavFLIP$_R$). (**d**) EAE was induced by injecting WT and vavFLIP$_R$ mice ($n = 11$) with the MOG_{35-55}-peptide and two further injections of pertussis toxin. Subsequently, the clinical score was monitored for 40 days. Data are pooled from two independent experiments and represented as the mean ± S.E.M. (**e**) WT and vavFLIP$_R$ animals were injected with the MOG_{35-55}-peptide in complete Freund's adjuvant. pLN cells isolated 11 (WT $n = 4$, vavFLIP$_R$ $n = 4$) and 14 (WT $n = 5$, vavFLIP$_R$ $n = 3$) days after injection were restimulated with the indicated concentrations of MOG peptide for 24 h, followed by flow cytometry analysis of IFN-γ, IL-17A and IL-4-producing T cells

autoantibodies were identified in sera from vavFLIP$_R$ mice compared with WT mice (Figure 7c).

Multiple organs can be affected in systemic autoimmune diseases. We therefore examined several organs from 1-year-old WT and vavFLIP$_R$ animals by histology. No differences between WT and vavFLIP$_R$ mice could be observed in brains, spleens and pancreas stained with haematoxylin and eosin (H&E) and in spleens stained for B cells and macrophages (data not shown). Kidneys from aged mice were stained with periodic acid–schiff (PAS) followed by histological scoring. The majority of glomeruli in kidneys from WT mice were normal (Figure 7d). In contrast, thickening of the Bowman's capsule and protein deposition in glomeruli were observed in kidneys from vavFLIP$_R$ mice, indicating nephropathy (Figure 7e). Glomerular deposition of PAS-positive material is common in aging mice.[39] However, significantly more tissue damage was detected in vavFLIP$_R$ kidneys with 63.6% of the kidney sections displaying a

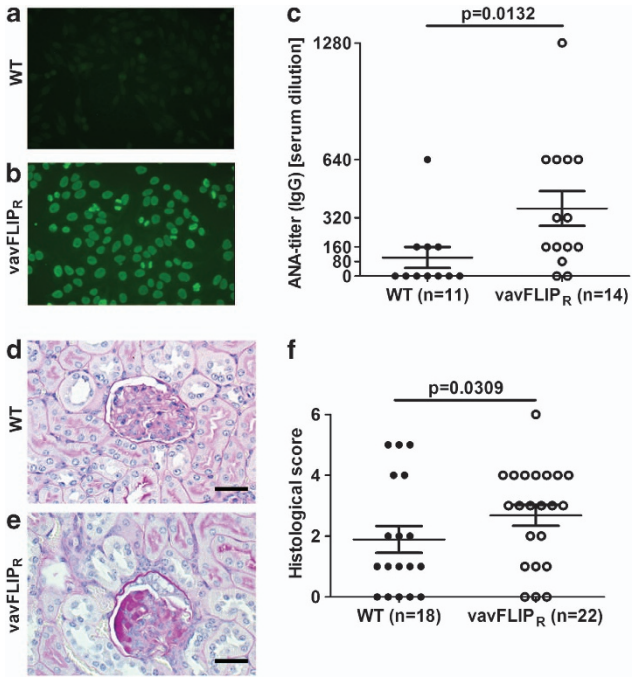

Figure 7 Autoantibody production and nephropathy in aged vavFLIP$_R$ mice. (**a**–**c**) Quantification of ANAs in sera from 1-year-old WT ($n=11$) and vavFLIP$_R$ ($n=14$) littermates. Representative examples of (**a**) negative fluorescent pattern (WT) and (**b**) homogenous ANA pattern (vavFLIP$_R$). The ANA-IgG titre is shown in (**c**). Symbols represent individual mice. Horizontal lines represent the mean; error bars display S.E.M. Statistical analysis was performed with two-tailed nonparametric Mann–Whitney *U*-test. (**d**–**f**) Kidneys from 1-year-old WT ($n=18$) and vavFLIP$_R$ ($n=22$) animals were analysed by histology. (**d** and **e**) Representative histological sections of paraffin-embedded kidneys stained with PAS are shown for (**d**) WT glomerulus with mild thickening of the Bowman's capsule and (**e**) vavFLIP$_R$ glomerulus with moderate thickening of the Bowman's capsule and moderate glomerular protein deposition. Scale bar represents 25 μm. (**f**) Histological score of PAS-stained kidneys. Individual mice are displayed as separate symbols. Horizontal lines represent the mean; error bars show S.E.M. Animals were divided up into groups of normal alterations (histological score <3) and moderate-to-severe alterations (histological score 3 or higher), followed by statistical analysis with Fisher's exact test

histological score of three or higher, implying mild-to-moderate alterations (Figure 7f). In comparison, only 27.8% of kidneys from WT mice manifested similar damage (Figure 7f). Thus, vavFLIP$_R$ mice have a greater degree of nephropathy compared with WT animals at 12–14 months of age.

The histological analyses of lungs from aged mice revealed that three of six vavFLIP$_R$ lungs stained with H&E displayed marked focal interstitial pneumonia compared with one of five WT lungs. Increase in bronchial-associated lymphoid tissue (BALT) has been described in aging mice.[40] Nevertheless, the amount of BALT was massively increased in four of six vavFLIP$_R$ animals (67%) in comparison with two of five WT mice (40%). Although the composition of BALT was not obviously altered, we detected more IgG-containing immune complexes (Figure 8). Infiltrating macrophages were observed in regions of interstitial pneumonia by immunohistochemical staining for B cells (B220), T cells (CD3) and macrophages (MAC2) in vavFLIP$_R$ lungs (Figure 8). Of note, interstitial pneumonia has occasionally been described for SLE.[41]

Taken together, the elevated levels of ANAs and tissue damage in kidneys and lungs are symptoms similar to human SLE.[41,42] Hence, the kidney damage may be related to the ANAs and represent a mild form of SLE nephropathy.

Discussion

CD95-mediated apoptosis has a crucial role in controlling immune responses and preventing autoimmune diseases.[1] c-FLIP proteins protect cells against CD95-induced apoptosis at the level of the DISC.[2] Although the isoforms c-FLIP$_L$ and c-FLIP$_S$ have been thoroughly characterised, not much is known about the functional role of c-FLIP$_R$ in the immune system. In this study, we report that constitutive expression of murine c-FLIP$_R$ results in altered lymphocyte populations and lupus-like symptoms with age.

Lpr and *gld* mice with mutations in the CD95 receptor and ligand, respectively, develop lymphoproliferative disease and autoimmunity with accumulation of unusual DN B220$^+$ T cells.[7,29,30,43] c-FLIP proteins inhibit the same apoptosis pathway by preventing caspase-8 cleavage at the DISC.[15,16] Indeed, T-cell-specific c-FLIP$_L$ transgenic mice were reported to develop autoimmunity when bred on Balb/c, but not C57BL/6, background.[25] However, neither altered Lpr nor accumulation of DN B220$^+$ T cells was identified in up to 1-year-old vavFLIP$_R$ mice, consistent with transgenic mice with T-cell-specific expression of murine c-FLIP$_L$ or human c-FLIP$_S$ in the C57BL/6 background.[26,27,31] Hence, neither constitutive expression nor overexpression of c-FLIP proteins, at least in the C57BL/6 background, is sufficient for recapitulation of the *lpr*/*gld* phenotype.

The autoimmune inflammation in EAE is mainly caused by autoreactive T$_H$1 and T$_H$17 effector cells.[37] *Lpr* mice showed a prolonged and enhanced inflammation in the central nervous system (CNS) upon EAE induction.[44] Hence, CD95/CD95L interactions are of importance to delete disease-initiating, autoreactive T cells in the CNS in the course of EAE. Both long and short c-FLIP isoforms have been reported to be upregulated in activated T cells from the cerebral spinal fluid in patients with active MS.[45,46] Interestingly, transgenic mice overexpressing human c-FLIP$_L$ were protected against EAE because of enhanced T$_H$2 effector responses and consequently reduced T$_H$1 effector responses.[38] Transgenic expression of murine c-FLIP$_R$ did not alter the cytokine production of T cells in a similar way, which may be one reason why the enforced expression of c-FLIP$_R$ only had a minor effect on the progression of EAE. Yu *et al.*[47] reported high expression levels of c-FLIP$_L$ in T$_H$17 cells, which protected these cells against AICD. This was proposed to be a mechanism for the high pathogenicity of T$_H$17 cells in autoimmune diseases. Expression levels of c-FLIP$_R$ in T$_H$17 cells was not investigated in this study, nevertheless, the increased expression of c-FLIP$_L$ in this cell population may override the effect of the constitutive c-FLIP$_R$ expression in vavFLIP$_R$ mice in the course of EAE. However, the impaired ability of naive vavFLIP$_R$ T cells to differentiate into the T$_H$17 subset *in vitro* and the minor reduction of effector T-cell responses observed in MOG-immunised vavFLIP$_R$ mice could possibly explain the slightly slower disease progression in vavFLIP$_R$ mice compared with WT littermates.

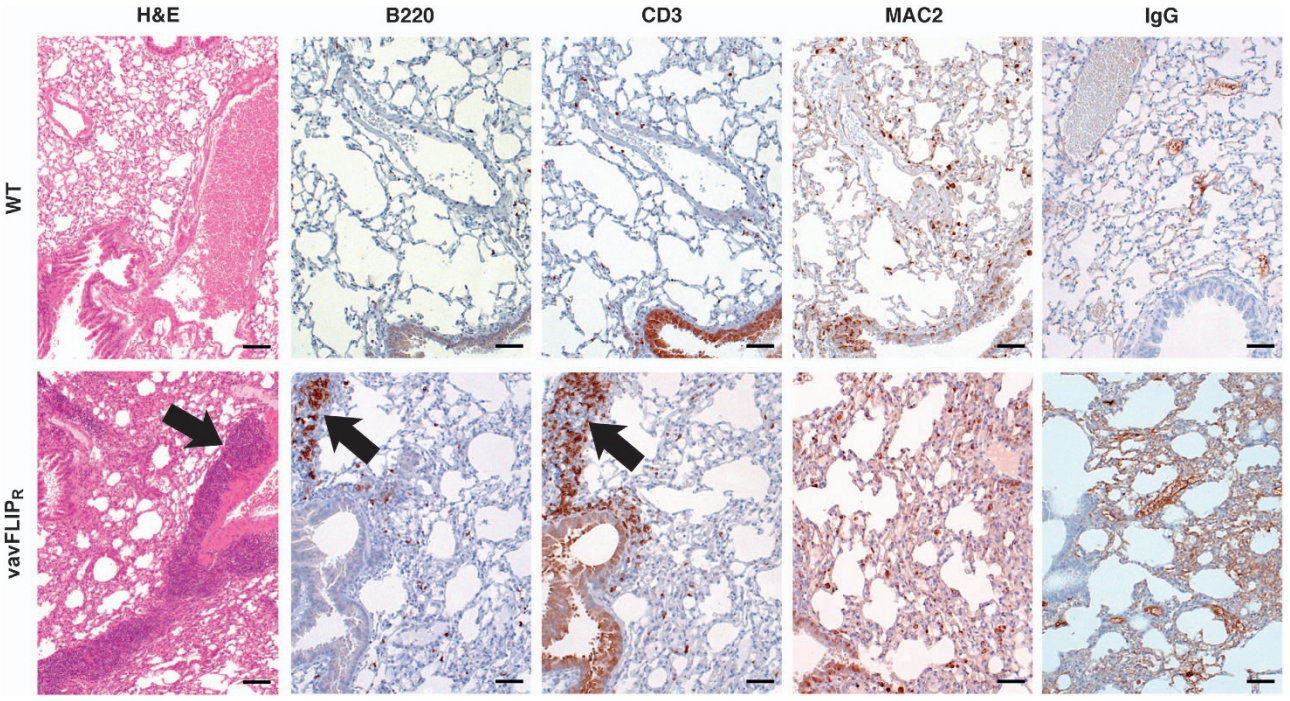

Figure 8 Histological alterations in lungs of aged vavFLIP$_R$ mice. Lungs were prepared from 1-year-old WT ($n=5$) and vavFLIP$_R$ ($n=6$) mice and paraffin embedded. Sections were stained with H&E, the B-cell marker B220, the T-cell marker CD3 and the macrophage marker MAC2, respectively. Deposition of IgG-containing immune complexes was detected with goat-anti-mouse antibodies. Representative tissue sections are shown. Arrows indicate increased BALT and interstitial pneumonia, respectively. Scale bars represents 200 μm for H&E section and 50 μm for all other sections

B- and T-cell numbers and distribution were normal in young vavFLIP$_R$ mice[28] and no differences in DCs, macrophages, granulocytes or NK cells could be identified even in mice at 1 year of age. Interestingly, aged vavFLIP$_R$ mice had altered lymphocyte populations with lower levels of T cells and higher frequencies of B cells compared with WT littermates. Moreover, reduced levels of CD8$^+$ cells were observed, which is consistent with a report of Wu *et al.*[48] where reduced peripheral CD8$^+$ cell numbers were described in mice with transgenic expression of the viral FLIP MC159 under control of the CD2 enhancer cassette. Furthermore, alterations in the ratio of antigen experienced to naive T cells were identified, most probably because of defective AICD. Human c-FLIP$_S$ is upregulated in the activation and expansion phase of an immune response, but is thereafter downregulated to enable AICD and elimination of effector T cells.[49] We previously described a similar kinetic for murine c-FLIP$_R$, which explains the defect in AICD upon constitutive c-FLIP$_R$ expression.[28] In this study, increased frequencies of activated T helper cells and antigen-experienced T cells as well as lower frequencies and numbers of naive T cells in vavFLIP$_R$ mice compared with WT mice were observed. This is consistent with a previous report where an increased memory T-cell pool was identified in c-FLIP$_S$ transgenic mice compared with WT animals after immunisation with the superantigen staphylococcal enterotoxin B.[27] Similarly to the activated T-cell phenotype, vavFLIP$_R$ B cells expressed activation markers to a higher extent than WT B cells. Strikingly, histological analyses of kidneys and lungs from 12 to 14 months old mice revealed a higher degree of nephropathy in vavFLIP$_R$ mice and a larger proportion of vavFLIP$_R$ animals displayed focal interstitial pneumonia and an increased amount of BALT compared with WT littermates. Moreover, elevated levels of anti-nuclear autoantibodies were identified in vavFLIP$_R$ sera, indicating that vavFLIP$_R$ mice develop a lupus-like phenotype with age. Hence, our findings imply that the altered lymphocyte populations with activated phenotypes in aged vavFLIP$_R$ mice are of functional relevance. Most probably the autoimmune disease observed in vavFLIP$_R$ animals is caused by a combination of autoreactive B and T cells, with persisting CD4$^+$ helper T cells, which may prime B cells to produce autoantibodies, and increased levels of B cells. In support of this notion, lupus-like disease was described in c-FLIP$_L$ transgenic mice on the Balb/c background and the development of autoimmunity in this study was shown to require CD4$^+$ T cells, which were proposed to result from impaired thymic selection.[25] Notably, elevated gene expression of *CFLAR* in CD33$^+$ myeloid cells, CD4$^+$ T cells and CD19$^+$ B cells was reported in SLE patients.[50] Furthermore, Xu *et al.*[51] observed that human lupus T cells did not downregulate c-FLIP$_S$ after initial activation, which suggests that c-FLIP proteins are of importance in the development of SLE disease. The higher level of T_{reg} cells in aged vavFLIP$_R$ mice is presumably a compensatory mechanism because of the observed autoimmunity. Imbalance of T_{reg} cells has been described in various autoimmune diseases.[52] Reduced levels or conflicting data have been reported in patients with, for example, juvenile idiopathic arthritis, autoimmune liver disease and myasthenia gravis.[52] Consistent with our findings, increased levels of T_{reg} cells were identified in patients with

primary Sjögren's syndrome[53] and in experimental arthritis in mice.[54] The expanded T_{reg} cell population observed in 1-year-old vavFLIP$_R$ animals most probably dampens the severity of the SLE-like phenotype.

We previously reported that vavFLIP$_R$ mice are better protected against *Listeria monocytogenes* infection compared with WT littermates.[28] Hence, c-FLIP$_R$ expression is beneficial in an acute infection, whereas we in this study demonstrate that chronic expression results in autoimmunity. To conclude, aged vavFLIP$_R$ mice have altered lymphocyte populations with increased levels of antigen-experienced T cells and higher activation status of both B and T cells. Moreover, these animals develop lupus-like symptoms with age. Our results show that c-FLIP$_R$ has an important role in the control of autoimmunity.

Materials and Methods

Mice. vavFLIP$_R$ mice were previously described.[28] WT littermates were used as control animals. All animals were kept in a specific pathogen-free environment in the animal facility of Helmholtz Centre for Infection Research, Braunschweig.[55] C57BL/6 mice were purchased from Harlan Laboratories (Indianapolis, IN, USA) and Charles River (Wilmington, MA, USA). MRL/*lpr* mice were a kind gift from Dr Detlef Neumann, Hannover Medical School, Hannover, Germany. All breeding and experiments were performed in accordance with the guidelines of national and local authorities.

Cell preparation. Lymphoid organs (pLNs, mesenteric lymph nodes, spleen and thymus) were isolated from mice killed via CO_2. Organs were homogenised through a 70 μm nylon mesh and washed with PBS. Erythrocytes were removed by 2-min incubation in ACK lysis buffer (0.15 M NH_4Cl, 1 mM $KHCO_3$, 0.1 mM EDTA, pH adjusted to 7.3 with NaOH) at room temperature followed by a further washing step. Primary murine cells were cultured in RPMI 1640 (Gibco – Life technologies, Grand Island, NY, USA) supplemented with 10% FCS (PAA, Pasching, Austria), 50 μg/ml of penicillin and streptomycin (Gibco – Life technologies), 1% non-essential amino acids (Gibco – Life technologies), 2 mM L-glutamine (Gibco – Life technologies) and 1 mM sodium pyruvate (Gibco – Life technologies).

***In vitro* generation of T helper cell subsets.** For differentiation of T helper subsets, $CD4^+CD62L^{high}CD25^-$ naive T cells were sorted by using a FACS Aria II (BD Biosciences, Heidelberg, Germany) or MoFlo (Beckman and Coulter, Indianapolis, IN, USA). Cells were seeded directly after sorting with 2×10^5 cells per well in 96-well plates and activated with plate-bound anti-CD3 and anti-CD28 in the presence of priming cytokines and inhibitory antibodies according to the respective T helper subset: T_H0: 2 μg/ml anti-CD3 (145-2C11, BioLegend, San Diego, CA, USA), 2 μg/ml anti-CD28 (37.51, BioLegend), 10 μg/ml anti-IL-4 (11B11, self-purified) and 10 μg/ml anti-IFN-γ (XMG1.2, self-purified); T_H1: 2 μg/ml anti-CD3 (145-2C11, BioLegend), 2 μg/ml anti-CD28 (37.51, BioLegend), 10 μg/ml anti-IL-4 (11B11, self-purified) and 10 ng/ml IL-12 (R&D Systems, Minneapolis, MN, USA); T_H17: 3 μg/ml anti-CD3 (145-2C11, BioLegend), 5 μg/ml anti-CD28 (37.51, BioLegend), 10 μg/ml anti-IL-2 (JES6-1A12, BioLegend), 10 μg/ml anti-IFN-γ (XMG1.2, self-purified), 2 ng/ml pTGF-β (R&D Systems), 30 ng/ml IL-6 (R&D Systems), 10 ng/ml IL-1-β (R&D Systems) and 20 ng/ml TNF-α (Preprotech, Rocky Hill, NJ, USA). T_H2 cells were differentiated as follows: $CD4^+CD62L^{high}CD25^-$ naive T cells were sorted as above. In all, 2×10^6 cells were seeded after sorting in 24-well plates and activated with plate-bound 5 μg/ml anti-CD3 (145-2C11, BioLegend) and 2 μg/ml anti-CD28 (37.51, BioLegend). After 3 days, 2×10^5 cells were transferred to 96-well plate in the presence of the following priming cytokines and inhibitory antibodies and cultured for additional 3 days: 10 ng/ml murine IL-2 (402-ML, R&D Systems), 10 ng/ml IL-4 (11B11, self-purified), 5 μg/ml anti-IFN-γ (XMG1.2, self-purified) and 5 μg/ml anti-IL12p40 (C17.8, R&D Systems). Subsequently, the differentiated cells were stained for CD4 and either IFN-γ, IL-4 or IL-17A (see staining procedure in the next paragraph) followed by flow cytometry analysis after 4 days of differentiation.

Flow cytometry. Cells were stained with Live/Dead near IR or blue fluorescent reactive dyes (Life Technologies) by incubation for 30 min in PBS at 4 °C. Thereafter, cells were washed and Fcγ III/II receptors were blocked by incubation with anti-CD16/CD32 (2.4G2, BD Biosciences). Subsequently, cells were washed and stained with antibodies in PBS containing 2% BSA for 20 min at 4 °C. The following antibodies were used: CD3-HorizonV450 (17A2), CD3-FITC (145-2C11), CD4-HorizonV500 (RM4-5), CD8-FITC (53-6.7), CD19-FITC (1D3), CD25-PE Cy7 (PC61.5) (all from BD Biosciences); CD4-Pacific Blue (RM4-5), CD8-APC (53-6.7), CD86-APC (GL-1), I-A/I-E-Alexa Fluor 700 (M5/114.15.2) (all from BioLegend); CD11c-APC eFluor780 (N418), CD19-PerCP Cy5.5 (1D3), CD44-PE (IM7), CD45R (B220)-APC (RA3-6B2), CD49b-APC (Dx5), CD62L-PerCP Cy5.5 (MEL-14), CD69-PE Cy7 (H1.2F3), F4/80-PE (BM8) and Gr1-Pacific Blue (RB6-8C5) (all from eBiosciences, San Diego, CA, USA). Samples were analysed by LSRII or LSRFortessa flow cytometers (BD Biosciences). The FlowJo software (TreeStar, Ashland, OR, USA) was used to analyse the data.

Intracellular proteins were stained after surface marker staining. For staining of Foxp3-Alexa Fluor 488, cells were fixed and permeabilised for intracellular cytokine staining by using the Foxp3 Staining Buffer Set (Miltenyi Biotec, Auburn, CA, USA) according to the manufacturer's protocol. For intracellular cytokine staining of IFN-γ-FITC (XMG1.2, BioLegend), IL-4-PE (11B11, eBioscience) and IL-17A-APC (eBio17B7, eBioscience), cells were stimulated for 4 h with PMA and ionomycin (Sigma Aldrich, Munich, Germany), with addition of Brefeldin A (Sigma Aldrich) for the last 2 h, before the staining was performed as for Foxp3.

Real-time detection PCR. cDNA was used as a template for real-time PCR using SYBR Green (Roche, Mannheim, Germany). Ubiquitin C (UBC) was used as reference gene for normalisation. Measurements were performed in duplicates in the LightCycler 96 system (Roche) using the following primers: UBC fwd 5′-AAGAGAATCCACAAGGAATTGAATG-3′; UBC rev 5′-CAACAGGACCTGCTGAACACTG-3′; IL4 fwd 5′-CATCGGCATTTTGAACGAG-3′; IL4 rev 5′-CGAGCTCACTCTCTGTGGTG-3′.

Experimental autoimmune encephalomyelitis. EAE was induced in 10–12 weeks old WT and vavFLIP$_R$ mice by injecting 200 μg MOG_{35-55}-peptide (MEVGWYRSPFSRVVHLYRNGK) together with 4 mg/ml mycobacteria in complete Freund's adjuvant subcutaneously at four sites. In all, 200 ng pertussis toxin was injected intraperitoneally to open the blood–brain-barrier. The pertussis toxin injection was repeated 2 days later. Mice were monitored daily for clinical signs of EAE from days 3 to 40 with 0 – no symptoms, 0.5 – partial limp tail, 1 – limp tail, 2 – delayed rotation from dorsal position, 2.5 – hindleg weakness, 3 – complete hindleg paralysis, 3.5 – starting foreleg weakness, 4 – paralysis of one foreleg, 5 – moribund, death. Mice with a score higher than 3 were killed.

For analysis of cytokine-producing T cells, mice were immunised with MOG_{35-55}-peptide as above, but without pertussis toxin to prevent the migration of primed T cells into the brain. pLNs were isolated from mice killed 11 and 14 days after injection. In all, 5×10^5 cells were seeded per well in 96-well plates and either left untreated or restimulated with plate-bound anti-CD3 (2 μg/ml; 145-2C11, BioLegend) and anti-CD28 (2 μg/ml; 37.51, BioLegend) or up to 50 μg/ml MOG_{35-55}-peptide for 24 h with addition of 10 μg/ml Brefeldin A (Sigma Aldrich) for the last 2 h. IFN-γ-, IL-4- and IL-17A-producing T cells were analysed by flow cytometry.

Analysis of ANAs. ANAs in sera from 1-year-old WT and vavFLIP$_R$ mice were analysed semiquantitatively by incubating HEp-2 cells seeded on microscope slides (Generic Assays, Dahlewitz, Germany) with sera diluted 1 : 80–1 : 1280 for 30 min at room temperature. Slides were washed two times 5 min in PBS followed by incubation with FITC-conjugated donkey anti-mouse IgG (Dianova, Hamburg, Germany) for 30 min in the dark. Thereafter, slides were washed two times 5 min in PBS, transferred to cover slips and sealed. Slides were analysed by fluorescence microscopy where a homogenous pattern was considered as positive for ANAs.

Histology. Kidneys, lungs, livers, spleens, pancreas and brains were isolated from 1-year-old WT and vavFLIP$_R$ mice. Organs were fixed in 4% neutrally buffered formaldehyde and embedded in paraffin for histological analysis. In all, 3 μm sections from organs were stained with H&E. The degree of focal interstitial pneumonia and BALT was determined in H&E-stained lung sections. Lungs were immunohistochemically stained with B220 (RA3-6B2; BD Biosciences), CD3 (SP7; Neo Markers, Fremont, CA, USA) and MAC2 (M3/38; CEDARLANE, Burlington, ON, Canada) to determine lymphocyte and macrophage infiltration. IgG complexes in lung sections were stained with goat-anti-mouse (TM-060-BN, Thermo Fisher Scientific, Waltham, MA, USA). Kidney sections were stained with PAS staining and the sections were analysed for thickening of the Bowman's capsule and

protein casts in glomeruli. Scoring was performed in a blinded manner for each criterion as follows: 0 – no alteration, 1 – low grade (slightly visible), 2 – moderate (clearly visible), 3 – severe (dominant finding). Scores were added to a total score for each organ.

Statistical analyses. Statistical analyses were performed by nonparametric Mann–Whitney *U*-test or Fisher's exact test using GraphPad Prism software (Graph Pad Software, La Jolla, CA, USA). Data are presented as the mean with S.E.M. and S.D. as error bars.

Conflict of Interest

The authors declare no conflict of interest.

Acknowledgements. We are grateful to Sabrina Schumann, Dominique Gollasch and Lena Seela for expert technical assistance, Anne-Marie Matthies for help with Ig ELISAs and Dr Marc Schuster for critically reading the manuscript. We thank Dr Detlef Neumann for providing us with MRL/*lpr* mice and Dr Jochen Huehn for various reagents. Moreover, we appreciate the excellent support from the FACS facility, especially Dr Lothar Groebe, and the animal facility, in particular David Dettbarn, at the Helmholtz Centre for Infection Research. We also thank Dr Frank Klawonn for assistance with statistical analyses. FE, MA and CP-S were supported by the President's Initiative and Networking Fund of the Helmholtz Association of German Research Centers (HGF) under contract number VH-GS-202. This project was funded by the DFG (SCHM1586/2-1 and SCHM1586/2-2).

1. Bouillet P, O'Reilly LA. CD95, BIM and T cell homeostasis. *Nat Rev Immunol* 2009; **9**: 514–519.
2. Krammer PH, Arnold R, Lavrik IN. Life and death in peripheral T cells. *Nat Rev Immunol* 2007; **7**: 532–542.
3. Alderson MR, Tough TW, Davis-Smith T, Braddy S, Falk B, Schooley KA *et al.* Fas ligand mediates activation-induced cell death in human T lymphocytes. *J Exp Med* 1995; **181**: 71–77.
4. Dhein J, Walczak H, Baumler C, Debatin KM, Krammer PH. Autocrine T-cell suicide mediated by APO-1/(Fas/CD95). *Nature* 1995; **373**: 438–441.
5. Brunner T, Mogil RJ, LaFace D, Yoo NJ, Mahboubi A, Echeverri F *et al.* Cell-autonomous Fas (CD95)/Fas-ligand interaction mediates activation-induced apoptosis in T-cell hybridomas. *Nature* 1995; **373**: 441–444.
6. Ju ST, Panka DJ, Cui H, Ettinger R, el-Khatib M, Sherr DH *et al.* Fas(CD95)/FasL interactions required for programmed cell death after T-cell activation. *Nature* 1995; **373**: 444–448.
7. Cohen PL, Eisenberg RA. Lpr and gld: single gene models of systemic autoimmunity and lymphoproliferative disease. *Annu Rev Immunol* 1991; **9**: 243–269.
8. Sneller MC, Straus SE, Jaffe ES, Jaffe JS, Fleisher TA, Stetler-Stevenson M *et al.* A novel lymphoproliferative/autoimmune syndrome resembling murine lpr/gld disease. *J Clin Invest* 1992; **90**: 334–341.
9. Peter ME, Krammer PH. The CD95(APO-1/Fas) DISC and beyond. *Cell Death Differ* 2003; **10**: 26–35.
10. Kischkel FC, Hellbardt S, Behrmann I, Germer M, Pawlita M, Krammer PH *et al.* Cytotoxicity-dependent APO-1 (Fas/CD95)-associated proteins form a death-inducing signaling complex (DISC) with the receptor. *EMBO J* 1995; **14**: 5579–5588.
11. Boatright KM, Renatus M, Scott FL, Sperandio S, Shin H, Pedersen IM *et al.* A unified model for apical caspase activation. *Mol Cell* 2003; **11**: 529–541.
12. Donepudi M, Mac Sweeney A, Briand C, Grutter MG. Insights into the regulatory mechanism for caspase-8 activation. *Mol Cell* 2003; **11**: 543–549.
13. Li J, Yuan J. Caspases in apoptosis and beyond. *Oncogene* 2008; **27**: 6194–6206.
14. Fischer U, Janicke RU, Schulze-Osthoff K. Many cuts to ruin: a comprehensive update of caspase substrates. *Cell Death Differ* 2003; **10**: 76–100.
15. Scaffidi C, Schmitz I, Krammer PH, Peter ME. The role of c-FLIP in modulation of CD95-induced apoptosis. *J Biol Chem* 1999; **274**: 1541–1548.
16. Krueger A, Schmitz I, Baumann S, Krammer PH, Kirchhoff S. Cellular FLICE-inhibitory protein splice variants inhibit different steps of caspase-8 activation at the CD95 death-inducing signaling complex. *J Biol Chem* 2001; **276**: 20633–20640.
17. Golks A, Brenner D, Fritsch C, Krammer PH, c-FLIPR Lavrik IN. a new regulator of death receptor-induced apoptosis. *J Biol Chem* 2005; **280**: 14507–14513.
18. Irmler M, Thome M, Hahne M, Schneider P, Hofmann K, Steiner V *et al.* Inhibition of death receptor signals by cellular FLIP. *Nature* 1997; **388**: 190–195.
19. Fuentes-Prior P, Salvesen GS. The protein structures that shape caspase activity, specificity, activation and inhibition. *Biochem J* 2004; **384**(Pt 2): 201–232.
20. Ueffing N, Singh KK, Christians A, Thorns C, Feller AC, Nagl F *et al.* A single nucleotide polymorphism determines protein isoform production of the human c-FLIP protein. *Blood* 2009; **114**: 572–579.
21. Ueffing N, Keil E, Freund C, Kuhne R, Schulze-Osthoff K, Schmitz I. Mutational analyses of c-FLIPR, the only murine short FLIP isoform, reveal requirements for DISC recruitment. *Cell Death Differ* 2008; **15**: 773–782.
22. Fricker N, Beaudouin J, Richter P, Eils R, Krammer PH, Lavrik IN. Model-based dissection of CD95 signaling dynamics reveals both a pro- and antiapoptotic role of c-FLIPL. *J Cell Biol* 2010; **190**: 377–389.
23. Micheau O, Thome M, Schneider P, Holler N, Tschopp J, Nicholson DW *et al.* The long form of FLIP is an activator of caspase-8 at the Fas death-inducing signaling complex. *J Biol Chem* 2002; **277**: 45162–45171.
24. Chang DW, Xing Z, Pan Y, Algeciras-Schimnich A, Barnhart BC, Yaish-Ohad S *et al.* c-FLIP(L) is a dual function regulator for caspase-8 activation and CD95-mediated apoptosis. *EMBO J* 2002; **21**: 3704–3714.
25. Qiao G, Li Z, Minto AW, Shia J, Yang L, Bao L *et al.* Altered thymic selection by overexpressing cellular FLICE inhibitory protein in T cells causes lupus-like syndrome in a BALB/c but not C57BL/6 strain. *Cell Death Differ* 2010; **17**: 522–533.
26. Hinshaw-Makepeace J, Huston G, Fortner KA, Russell JQ, Holoch D, Swain S *et al.* c-FLIP(S) reduces activation of caspase and NF-kappaB pathways and decreases T cell survival. *Eur J Immunol* 2008; **38**: 54–63.
27. Oehme I, Neumann F, Bosser S, Zornig M. Transgenic overexpression of the Caspase-8 inhibitor FLIP(short) leads to impaired T cell proliferation and an increased memory T cell pool after staphylococcal enterotoxin B injection. *Eur J Immunol* 2005; **35**: 1240–1249.
28. Telieps T, Ewald F, Gereke M, Annemann M, Rauter Y, Schuster M *et al.* Cellular-FLIP, Raji isoform (c-FLIPR) modulates cell death induction upon T-cell activation and infection. *Eur J Immunol* 2013; **43**: 1499–1510.
29. Watanabe-Fukunaga R, Brannan CI, Copeland NG, Jenkins NA, Nagata S. Lymphoproliferation disorder in mice explained by defects in Fas antigen that mediates apoptosis. *Nature* 1992; **356**: 314–317.
30. Yasutomo K, Maeda K, Nagata S, Nagasawa H, Okada K, Good RA *et al.* Defective T cells from gld mice play a pivotal role in development of Thy-1.2 + B220 + cells and autoimmunity. *J Immunol* 1994; **153**: 5855–5864.
31. Lens SM, Kataoka T, Fortner KA, Tinel A, Ferrero I, MacDonald RH *et al.* The caspase 8 inhibitor c-FLIP(L) modulates T-cell receptor-induced proliferation but not activation-induced cell death of lymphocytes. *Mol Cell Biol* 2002; **22**: 5419–5433.
32. Leverkus M, Walczak H, McLellan A, Fries HW, Terbeck G, Brocker EB *et al.* Maturation of dendritic cells leads to up-regulation of cellular FLICE-inhibitory protein and concomitant down-regulation of death ligand-mediated apoptosis. *Blood* 2000; **96**: 2628–2631.
33. Huang QQ, Perlman H, Huang Z, Birkett R, Kan L, Agrawal H *et al.* FLIP: a novel regulator of macrophage differentiation and granulocyte homeostasis. *Blood* 2010; **116**: 4968–4977.
34. Sakaguchi S. Regulatory T cells: key controllers of immunologic self-tolerance. *Cell* 2000; **101**: 455–458.
35. Hori S, Nomura T, Sakaguchi S. Control of regulatory T cell development by the transcription factor Foxp3. *Science* 2003; **299**: 1057–1061.
36. Iglesias A, Bauer J, Litzenburger T, Schubart A, Linington C. T- and B-cell responses to myelin oligodendrocyte glycoprotein in experimental autoimmune encephalomyelitis and multiple sclerosis. *Glia* 2001; **36**: 220–234.
37. Fletcher JM, Lalor SJ, Sweeney CM, Tubridy N, Mills KH. T cells in multiple sclerosis and experimental autoimmune encephalomyelitis. *Clin Exp Immunol* 2010; **162**: 1–11.
38. Tseveleki V, Bauer J, Taoufik E, Ruan C, Leondiadis L, Haralambous S *et al.* Cellular FLIP (long isoform) overexpression in T cells drives Th2 effector responses and promotes immunoregulation in experimental autoimmune encephalomyelitis. *J Immunol* 2004; **173**: 6619–6626.
39. Maronpot RR BG, Gaul BW. *Pathology of the Mouse.* Cache River Press: St Louis, MO, USA, 1999, p 699.
40. Pettan-Brewer C, Treuting PM. Practical pathology of aging mice. *Pathobiol Aging Age Related Dis* 2011; **1**: doi:10.3402/pba.v1i0.7202.
41. Cheema GS, Quismorio FP Jr. Interstitial lung disease in systemic lupus erythematosus. *Curr Opin Pulm Med* 2000; **6**: 424–429.
42. Munoz LE, Gaipl US, Franz S, Sheriff A, Voll RE, Kalden JR *et al.* SLE–a disease of clearance deficiency? *Rheumatology (Oxford)* 2005; **44**: 1101–1107.
43. Budd RC, Van Houten N, Clements J, Mixter PF. Parallels in T lymphocyte development between lpr and normal mice. *Semin Immunol* 1994; **6**: 43–48.
44. Suvannavejh GC, Dal Canto MC, Matis LA, Miller SD. Fas-mediated apoptosis in clinical remissions of relapsing experimental autoimmune encephalomyelitis. *J Clin Invest* 2000; **105**: 223–231.
45. Sharief MK. Increased cellular expression of the caspase inhibitor FLIP in intrathecal lymphocytes from patients with multiple sclerosis. *J Neuroimmunol* 2000; **111**: 203–209.
46. Semra YK, Seidi OA, Sharief MK. Overexpression of the apoptosis inhibitor FLIP in T cells correlates with disease activity in multiple sclerosis. *J Neuroimmunol* 2001; **113**: 268–274.
47. Yu Y, Iclozan C, Yamazaki T, Yang X, Anasetti C, Dong C *et al.* Abundant c-Fas-associated death domain-like interleukin-1-converting enzyme inhibitory protein expression determines resistance of T helper 17 cells to activation-induced cell death. *Blood* 2009; **114**: 1026–1028.

48. Wu Z, Roberts M, Porter M, Walker F, Wherry EJ, Kelly J *et al.* Viral FLIP impairs survival of activated T cells and generation of CD8+ T cell memory. *J Immunol* 2004; **172**: 6313–6323.
49. Kirchhoff S, Muller WW, Li-Weber M, Krammer PH. Up-regulation of c-FLIPshort and reduction of activation-induced cell death in CD28-costimulated human T cells. *Eur J Immunol* 2000; **30**: 2765–2774.
50. Hutcheson J, Scatizzi JC, Siddiqui AM, Haines GK 3rd, Wu T, Li QZ *et al.* Combined deficiency of proapoptotic regulators Bim and Fas results in the early onset of systemic autoimmunity. *Immunity* 2008; **28**: 206–217.
51. Xu L, Zhang L, Yi Y, Kang HK, Datta SK. Human lupus T cells resist inactivation and escape death by upregulating COX-2. *Nat Med* 2004; **10**: 411–415.
52. Dejaco C, Duftner C, Grubeck-Loebenstein B, Schirmer M. Imbalance of regulatory T cells in human autoimmune diseases. *Immunology* 2006; **117**: 289–300.
53. Gottenberg JE, Lavie F, Abbed K, Gasnault J, Le Nevot E, Delfraissy JF *et al.* CD4 CD25high regulatory T cells are not impaired in patients with primary Sjogren's syndrome. *J Autoimmun* 2005; **24**: 235–242.
54. Monte K, Wilson C, Shih FF. Increased number and function of FoxP3 regulatory T cells during experimental arthritis. *Arthritis Rheum* 2008; **58**: 3730–3741.
55. Stehr M, Greweling MC, Tischer S, Singh M, Blocker H, Monner DA *et al.* Charles River altered Schaedler flora (CRASF) remained stable for four years in a mouse colony housed in individually ventilated cages. *Lab Anim* 2009; **43**: 362–370.

Supplementary Information accompanies this paper on Cell Death and Disease website (http://www.nature.com/cddis)